Mining Science, vol. 30, 2023, 113–133

www.miningscience.pwr.edu.pl

Mining Science

(Previously Prace Naukowe Instytutu Gornictwa Politechniki Wroclawskiej, ISSN 0370-0798)

ISSN 2300-9586 (print)
ISSN 2353-5423 (online)

Received February 24, 2023; Reviewed; Accepted September 25, 2023

APPLICATION OF TERRESTRIAL LASER SCANNING FOR THE EVALUATION OF GEOKINEMATICS OF SELECTED STRUCTURAL PHENOMENA IN MINE WORKINGS IN THE RUDNA MINE (SW POLAND)

Dominik SOKALSKI[1, 2]*, Jurand WOJEWODA[3]

[1] University of Wroclaw, Institute of Geological Sciences, Maxa Borna 9, 50-204 Wroclaw
[2] KGHM Polska Miedź S.A., Marii Skłodowskiej-Curie 48, 59-301 Lubin
[3] Wrocław University of Science and Technology, Na Grobli 15, 50-421 Wrocław

Abstract: A series of terrestrial laser scanner measurements were made at selected sites of the Rudna mine. Using the method of differential images, the applicability of scanning was demonstrated for the recognition of the deformations taking place and the destruction of post-mining voids in the rock mass. At the same time, the usefulness of the technique used for the documentation of tectonic phenomena, practically invisible with classical methods of geological documentation, was demonstrated. The structure discovered by the authors, tectonic elongated-helicoidal asymmetric gouge (TEHAG), documents the process of horizontal and parallel to layering tectonic dislocations of rocks.

Keywords*: *Rudna mine, terrestrial laser scanning, induced fractures, structural phenomena

1. INTRODUCTION

The Rudna mine extracts copper-silver ore, which is hosted in rocks formed in the European Permian Basin (Van Wees et al. 2000). Polymetallic mineralization was formed as a result of a long and multi-stage process and is associated primarily with the

* Corresponding author: dominik.sokalski@uwr.edu.pl (D. Sokalski)

doi: 10.37190/msc233007

Kupferschiefer, which forms an almost continuous layer not only in the area of the deposit, but also within the entire basin (Vaughan et al. 1989; Oszczepalski 1999; Piestrzynski (ed.) 2007). In recent years, the mining operations are being conducted deeper due to the monoclinal inclination of the rocks towards the north, and currently reaches about 1300 meters below ground level. The deposit is not strictly bounded to only copper-bearing shale and also occurs in rocks under and above it. A typical tri-partite deposit profile is formed by (from below): (1) sandstones of the Weissliegend, copper--bearing, (2) clayey-bituminous shale, and (3) the Zechstein dolomitic limestone (Piestrzynski, Wodzicki 2000; Piestrzyński (ed.) 2007). However, mine geologists distinguish 16 lithofacial varieties, which is important for production and technological processes (Kaczmarek et al. 2017; Twardowski 2023).

Monitoring of active structures is an important part of the mine operations. Mine geologists are tasked with documenting the structure of the deposit, including potential geohazards, which is also very important for the safety of mining operations. In the southern part of the mining area, the blocky structure of the rock mass caused significant water hazards, making it difficult to proceed with mine openings. New type of danger emerged as the mining fields were going toward the north to greater depths. At present, gas-geodynamic hazards are also appearing, resulting from, among other things, the rock mass structure, and thus their prediction is becoming particularly important for mining safety. Exploitation process makes local and regional tectonic deformation, overlapped with non-tectonic damage. While the room-and-pillar mining system and the maintenance of an appropriate geometry of pillars prevents the destruction of mine workings due to convergence. The damage of pillars themselves is associated with the formation of local fractures, including so-called induced fractures (sensu Ollier 1978; Wojewoda, Ollier, 2012). Their formation, development, and geometry, most often depend on the local shape of the pillar. In some pillars, their corners are the first to be destroyed, and the propagation of fractures depends on the lithology of the rocks building the pillars. The progress and monitoring of such non-tectonic processes, is possible by measuring the deformation state of the rock mass at the time of measurement in successive time epochs.

Previous studies have shown that terrestrial laser scanning is an excellent tool for recording and identifying structural phenomena (Sokalski 2022, Sokalski et al. 2019, 2020). This method is particularly useful in the documentation of underground mine workings, where conditions are difficult and a single visit to the site is limited in time. The method has already been used for many years by mine surveyors for, e.g., inventorying mining infrastructure, designing and modeling workings deformation, or surveying hard-to-reach areas (Dusza-Pilarz, Kirej 2019; Kumosiński Patykowski 2020; Marzec et al. 2016; Patykowski, Kumosiński 2014; Patykowski et al. 2013). So far, it has not been applied to geological documentation and monitoring of geodynamic processes in the conditions of KGHM mines (see, e.g., Slaker 2015).

2. RESEARCH THESIS

The main objective of the conducted research was to confirm the suitability of laser scanning for documentation of structural phenomena and process inference. For that purpose, tests of the device were performed on selected sites in order to select optimal scanning parameters. In the two further presented sites, scanning was repeated several times, which allowed precise mapping of the rock mass structure, including discontinuity surfaces. Making such detailed documentation in mine workings would be difficult to achieve with observations made using traditional field methods.

3. OUTLINE OF THE GEOLOGICAL STRUCTURE OF THE DEPOSIT AREA

3.1. PALEOGEOGRAPHY AND LITHOGENESIS

KGHM's deposit area is located within the Fore-Sudetic Monocline, although the correct name for a geological structural unit of this type should be Homocline (Neuendorf et al. 2005; Żelaźniewiecz et al. 2011). The unit is formed of Permian and Mesozoic sedimentary rocks, the layering of which is inclined at an angle from 30 to 60 in a northeasterly direction. Such an alignment of rocks is related to the geodynamic remodeling of the area. The pelogeography and geological history of the deposit area has been described by many authors (including Konstatynowicz (ed.) 1971; Klapcinski et al. 1984; Piestrzyński (ed.), 1996; 2007).

In the Early Permian, this part of the homocline was land, where plain-river sedimentation dominated, which transitioned to land-period-lake sedimentation towards the north. That's when today's red-rock sediments and the Walchia shale were formed. In most of the Polish part of the basin appeared dune areas – paleoergs. At the turn of the Early and Late Permian, the area was flooded by a shallow sea (the Zechstein Sea). From this period are preserved relics of paleodunes, partially eroded by the sea, which in present-day mining practice are called elevations (see Fig. 1), and are built of sandstones of the Weissliegend – a discolored part of the Rotliegend (Kiersnowski 1995; Kiersnowski et al. 2010; Papiernik et al. 2010; Nemec, Porębki 1977; Śliwiński 2000; Karnkowski 2007).

In the Late Permian, the basin deepened and pelagic clayey-marly sediments were formed, highly enriched in organic matter (Oszczepalski 1999; cf. Kaczmarek 2006; Śliwinski 2000). Later, cyclic changes in sea level resulted in the formation of evaporite sediments – carbonates, anhydrites and salts (evaporite cyclothems). Seven such cycles have been described in the European Permian Basin, although only four of them are present in the deposit area – PZ1, PZ2, PZ3 and PZ4. Only the lowest of these (PZ1) shows the most complete profile, and mineralized zone is associated with it. The Fore-Sudetic the southern boundary between Fore-Sudetic Homocline and crystalline and metamorphosed Precambrian and Old Paleozoic rocks of the Fore-Sudetic Block is

formed by the Middle Odra Fault Zone oriented at ca. WNW–ESE (Konstantynowicz (ed.) 1971; Oberc 1967; 1972).

3.2. STRUCTURAL CHARACTERISTICS

The southern part of the deposit area is dominated by faults of the same orientation as in the Middle Odra Fault Zone (WNW–ESE). The faults form zones composed of a series of parallel, oblique, and en echelon faults. Horsts, grabens and staircase systems have been distinguished (e.g., Piestrzynski (ed.) 2007). In the central part of the deposit, two, almost parallel, fault zones are marked – the Biedrzychowa and Rudna Główna Fault Zones, both normal-strike slip fault zones, which end in "horsetail" type structures (Markiewicz et. al. 1995). The Trzebcz-Polkowice and Paulinów fault zones with the WSW–ENE orientation of the main structures form a cross-cut system of NE–SW and NW-SE intersecting faults with down-slip up to a dozens of meters (see Fig. 1).

Fig. 1. Overview map of the Rudna mining area against the background of the elevation zones of the top of the Weissliegend (dashed blue), identified tectonic structures and the (red lines) outline of the mine workings (black lines); explanations of abbreviations: ECR – Central Elevation of Rudna, ENR – Northern Elevation of Rudna, ET – Tarnówek Elevation, EZM – Żelazny Most Elevation; RGFZ – Rudna Główna Fault Zone, BFZ – Biedrzychova Fault Zone, TPFZ – Trzebcz-Polkowice Fault Zone, PFZ – Paulinów Fault Zone; R-IX, R-XI – location of shafts)

Observations from mine workings prove that most of the structures in the lower part of the Zechstein were formed as mid-layer deformations (Piestrzynski (ed.) 2007). Folds and detachments are most numerous within the copper-bearing shale. Displacements with a large horizontal component are common in the bituminous shale (e.g., Dumicz, Don 1977). Slickenslides also occur on the surfaces of layering in dolomite (Salski 1975). Commonly occurring deformations showing intralayer displacements document a thrusting dislocation "upward toward NE".

Lithology affects the shear susceptibility, hence the variation in the development of structures (including faults, the arrangement and density of fractures and stylolithization) within individual sandstone and carbonate lithofacies (cf. Piestrzynski (ed.) 2007). In the Rudna mine, the NNW-SSE direction of fractures in the carbonates is dominant, and a common phenomenon in these formations is the occurrence of gently sloping fractures (less than 30°) which are associated with layering parallel faults that have formed as a result of horizontal displacement in the bottom part of Ca1 series (Markiewicz et al. 1995). In the central part of the deposit, intensive faulting locally lead to an increase in inclination of up to 20°.

In spite of long-wavelength folds with NW-SE oriented axes (Piestrzynski (ed.) 1996), over the faults some flexures were also formed. These structures are found in all parts of the deposit area, including within the Paulinów, Rudna Główna and Jakubów fault zones (Fig. 1, Markiewicz et al. 1995). In the central part of the deposit, the most significant zone is the Rudna Główna Fault Zone, which is responsible for many local geodynamic phenomena. Associated with it are three parallel fault zones oblique to it: the Biedrzychowa, Trzebcz-Polkowice and Paulinów fault zones (Fig. 1). The width of these zones locally reaches up to about 500 m. The Pualinów Fault Zone (also called Paulinów Syncline) is accompanied by numerous faults running obliquely, parallel or perpendicular to the main strike of the structure. They have varying orientation, component of movement and throw values (Selerowicz 2011). The entire structure is also crossed by lower-order faults parallel to the Rudna Główna Fault Zone. Some of the faults parallel to the axis of the syncline have a sigmoidal shape, which relates to the boundaries of the syncline. This allows us to assume that within the structure there was a sliding movement with the direction: the NNW hanging wall towards the WSW and the SSE footwall towards the ENE. Such an alignment is observed within the elevation zones, while in the depressions the faults run in a direction parallel to the syncline, which may suggest the influence of paleomorpholgy on the observed deformation (op. cit.).

3.3. AREA COVERED BY THE EXPERIMENT

In this work, we present the results of scanning at two sites that are considerably distant from each other and differ in the profile of the rocks observed in the mine workings.

The first site is located on the northern slope of the Northern Elevation of Rudna, about 1 km to the NW of the R-IX shaft (for location see Fig. 1). The profile of the rocks found in the workings is similar to the typical one: in the bottom of the pit there is a clayey sandstone overlying bituminous and dolomitic shale, with a total thickness of 0.5 m of the shale. The dolomitic shale transitions smoothly into a several-centimeter--thick clay dolomite, overlied by the banded dolomite, which reaches the roof of the excavation. Within it were identified surfaces of curved, dipping at a slight angle of less than 30° fractures forming a "trough" structure with an axis oriented in the NNE-SSW direction. The structure is revealed on the opposing walls of the mine working and in the opening perpendicular to it. The site is located approx. 150 m from the northern boundary of the Paulinów Fault Zone.

The second site is located within the Elevation of the Żelazny Most, about 1 km to the W from the R-XI shaft (for location see Fig. 1). In the excavation, practically all the height of the wall there is anhydritic sandstone, over which there is a thin layer of bituminous shale of a thickness of 2 cm. Beneath the very roof is a thin layer of sandy or banded dolomite, about 10 cm thick. Despite the relatively close proximity to the southern boundary of the Paulinów Fault Zone (about 220 m), no significant tectonic structures were observed in the immediate vicinity of the site, except for isolated fractures in the roof of the mine workings.

4. METHOD OF MEASUREMENT EXPERIMENT

The sites were initially accessed, documented and recognized in terms of both sedimentological and structural-tectonic features of the rocks. The lithological profiles were described, and oriented samples were additionally taken for petrographic and microstructural studies in the case of the second site. The marker surfaces of discontinuities were measured with a geological compass. Photographic documentation was also made.

Before beginning their research in the mine workings, the authors had considered using photogrammetry to record structural damage to the rock mass, but this intent was waived for logistical reasons. Proper (and repeatable in use) illumination of the site would have required the involvement of additional staff and equipment, for which the authors did not obtain permission. Due to the challenging conditions in the mine workings of the Rudna mine and the resulting severely limited time underground, the authors decided on a more resistant to difficult conditions and more time-efficient method of laser scanning.

Laser scanning is a non-invasive and very fast method of acquiring spatial data for documentation and survey purposes, which is now used in a very wide range of applications: from underground and open-pit mining, construction and architecture, to forestry and forensics. The scanner measures distance using a laser beam that reflects off the object and returns to the device. The parameters that are recorded are mainly the

angles of the emitted laser beam, the distance to the object and the power of the reflected signal. They depend on a number of factors, e.g., atmospheric conditions, dust, the nature of the scanned surfaces, their humidity, or position relative to the scanner. As a result of the measurement, a cloud of points is generated, each having its own spatial coordinates. Objects in the scanned space are analyzed, and information about their geometry, color and reflection intensity is recorded for each point in the cloud (Dronszczyk, Strach 2016).

The devices available on the market differ primarily in the method of distance measurement, which directly impacts the range, speed of operation and precision (resolution) of measurement of a given device. There are pulsed scanners, which generally, are slightly less accurate and slower in operation, but offer a greater range (up to several km), and phase scanners, which are characterized by greater precision and speed, however, their range is significantly smaller (up to several hundred m).

Spatial measurements were made with a Riegl VZ400i pulse type terrestrial laser scanner. Several other devices of a similar class were tested prior to the measurements, but the functionality of the chosen device (e.g., ability to work for a long time at relatively high temperatures, dust resistance, high tolerance to moisture found in the mine atomosphere and side walls), as well as visualization and interpretation features of the dedicated software demonstrated the best suitability for analyzing structural phenomena.

The two selected sites are located in mine workings of similar geometry. Measured phenomena were observed at pillars' corners or at the opposing walls of mine workings. In order to obtain a dense point cloud, scanning was carried out at the maximum frequency of the laser pulse (1200 kHz). Very high mapping accuracy along the entire length of the object was achieved by scanning from several intermediate stations, spaced densely enough (less than 5 m apart) so that the point cloud covers the object completely. Reference targets often used to combine scans were not used for registration. The registration process was performed in two stages: (1) automatic registration based on all parameters from the scanner sensors and stored in the data for each sub-station, as well as on the basis of voxels created from the point clouds, the size of which was selected automatically based on the analysis of the point cloud and the established characteristics of the object (e.g., closed, irregular volume). The registration error (expressed in standard deviation) measured few cm after this step for each site; (2) fitting plane patches generated on the basis of given parameters (such as: minimum point count, maximum standard deviation, maximum deviation, minimum reflectance) from individual point clouds, which is then improved in an iterative process whose parameters were changed step by step until the minimum error (expressed in standard deviation) was achieved. After this step it measured 2–3 mm in both sites.

At the first test site, cyclic scanning was carried out to observe damage to technological pillars located outside the mining fields over time. Ten series of measurements were made over a period of 18 months. Each series was performed with identical settings of scanning parameters and with identical placement of intermediate stations.

After recording of each measurement series, the data were filtered by the attributes of the returning laser beam (reflectance, deviation) and to simplify the structure of the point cloud (octree filter). Some parts of the point cloud were additionally filtered for structural analysis purposes and to apply advanced 3D visualization effects (transparency of points), which allow, e.g., to observe the bottom of mine workings through points corresponding to the roof and vice versa, but also allow for better visualization of details in side walls. The raw and processed data after registration and basic filtering take up more than 200 GB of storage space.

The registered point cloud from a single measurement series has 650 million points, and after aligning all series into a single project for differential imagery, the complete point cloud has almost 7 billion points. Registration of successive measurement series was carried out using the same method as registering scans from sub-stations (iterative process of alignment based on fitting of plane patches). The registration error (expressed as standard deviation) for a project consisting of 10 measurement epochs reached 4 mm.

The mine workings at the Rudna mine are subject to continuous deformation of varying intensity and source. Deformations/displacements in the described objects are analyzed in an eminently local reference system. Algorithms used in the registration process use plane patches generated from all point clouds (corresponding to each measurement epochs), that have positions in the measurement space that fit throughout the measurement period (i.e., 18 months). An iterative process that compares fitting plane patches generally reduces the number of fitting planes (by narrowing, e.g., the radius of search for plane patches and reducing the value of standard deviation), however, at the end of the registration process, there were identified more than 50 000 fitting plane patches for site no. 1 and over 20 000 for site no. 2. In underground mine workings, alignment of clouds on the basis of such plane patches gives much better results than alignment of clouds on reference targets. Also a control of iterative process parameters guarantees that even if the entire excavation is subject to deformation, in a very locally measured object the measured displacements are independent of the displacements of the surrounding rock-mass.

5. MEASUREMENTS AND RESULTS

5.1. INDUCED FRACTURES

The entire crossing of the mine workings was scanned, while a section of the point cloud with a fragment of a pillar corner, in which induced fractures have developed, was analyzed in detail. Two discontinuity surfaces with orientations approximately parallel to the wall divide the corner built of anhydritic sandstone into three elongated blocks about 10 cm wide and up to 75 cm high, which are marked I, II and III in Fig. 2. The illustration juxtaposes a perpendicular view to the fracture surfaces in a photo taken with a traditional

camera and the same section of the excavation recorded as a point cloud. The white outline indicates the section of the cloud that was compared on the differential scans.

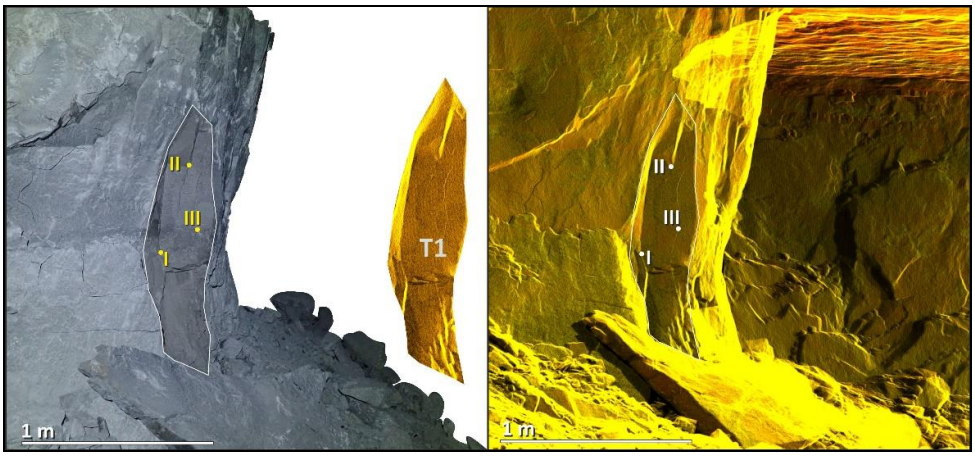

Fig. 2. View of the pillar corner with identified induced fractures (I, II, III) in site 1; comparison of the view in the photographic image (on the left) and the point cloud from laser scanning (on the right); both taken at the time of recording the first measurement series (T1). Despite not using a flash, the use of which flattens three-dimensional objects in the photograph, the differences in the depth of the image and the detail of the documentation of the site taken through digital photography and laser scanning are clearly visible. The scale was precisely measured in the point cloud and then duplicated in the digital photograph, it is for illustrative purposes only to show the size of the analyzed object. The image on the left was taken in a position perpendicular to the study object. The image on the right was shown in orthogonal projection

The differential scan formed by combining series of ten measurement was analyzed. Displacement kinematics was analyzed in two cross sections perpendicular to the fracture surfaces, corresponding to projections of the point cloud on two planes. Figure 3 presents the front projections, corresponding to the projection on a plane parallel to the face of the pillar corner.

Figure 4, on the other hand, presents top projections on a plane that intersects the zone of fractures horizontally. To increase the number of visualized points, the plane cutting the cloud was assumed to be 5 mm thick. Therefore, the plane established was moved across the entire height of the wall with particular attention to the analyzed fracture zone. The initial state represents a section from the first measurement series (T1) recorded in March 2020. Overlaying the subsequent measurement series T2 and T3 on the T1 scan in the front view reveals the distinction of the individual blocks (Figs. 3a, 3b), but no manifestation of movement is observed in the top view. With each successive measurement series, a general movement of the wall into the interior of the mine working is observed, which is visible not only in the fragment with the corner, but within the entire northwestern wall. In the next measurement series (T4), the progressive inward movement of the wall is

made apparent (Fig. 3c), but the first differentiation in the movement of individual blocks is also indicated in the top view, with Blocks II and III moving to the SE, and

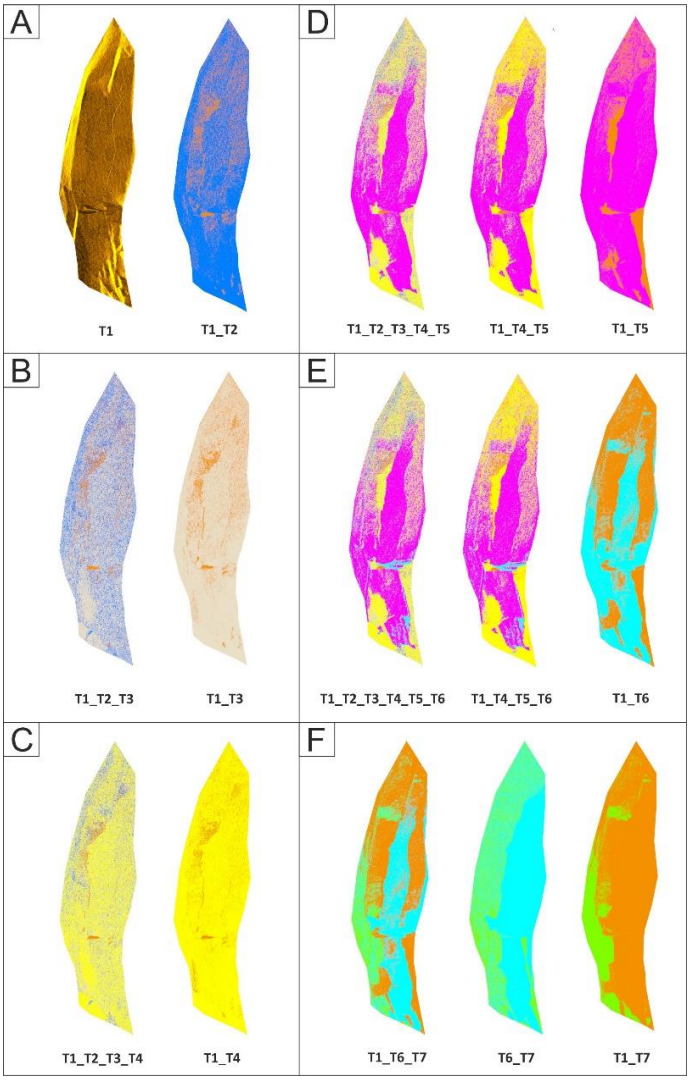

Fig. 3. Comparison of differential images documenting subsequent stages of development of induced fractures (for explanation, see subsection Measurements and results – induced fractures). The individual colors represent individual measurement epochs, which, when superimposed, produce differential images created by detaching and attaching selected measurement epochs. The selected measurement epochs have been superimposed in order to best visualize the destruction process. The selected measurement epochs were superimposed so as to best visualize the destruction process. The colors correspond to each measurement epoch: T1 – orange, T2 – blue, T3 – beige, T4 – yellow, T5 – fuchsia, T6 – aqua, T7 – green

a crack opening between them (Fig. 4a). In the front view, the lowering of Block II and III relative to Block I and the rock mass is evident. A noticeable differentiation becomes apparent on a differential scan consisting of five measurement series. A distinct displacement of Block II towards the SE and a widening of the fracture between Block I and Blocks II and III are marked, as well as a few milimeters lowering of Blocks II and III towards the bottom of the excavation (Fig. 3d). The juxtaposition of the differential scan from T1 to T6 in the front view reveals a distinct lowering of Blocks II and III toward the bottom and an enlargement of the fractures between the rock mass and Block I and between Blocks II and III (Fig. 3e). The top view shows the process of fracture opening between Block I and Block II, as well as the displacement of Block II towards the SE, and Block III in the opposite direction towards the NW (Fig. 4b). In the differential image for the seven series from T1 to T7, the key moment is recorded, when the failure occurred by breaking Block II and Block III from Block I (Fig. 3f). A new wall surface was created along the fracture between Block I and Block II (Fig. 4c). At the same time, the expansion of the fracture between the rock mass and Block I is recorded in the top view on the differential scan for consecutive measurement series (from T7 to T10) (Fig. 4d).

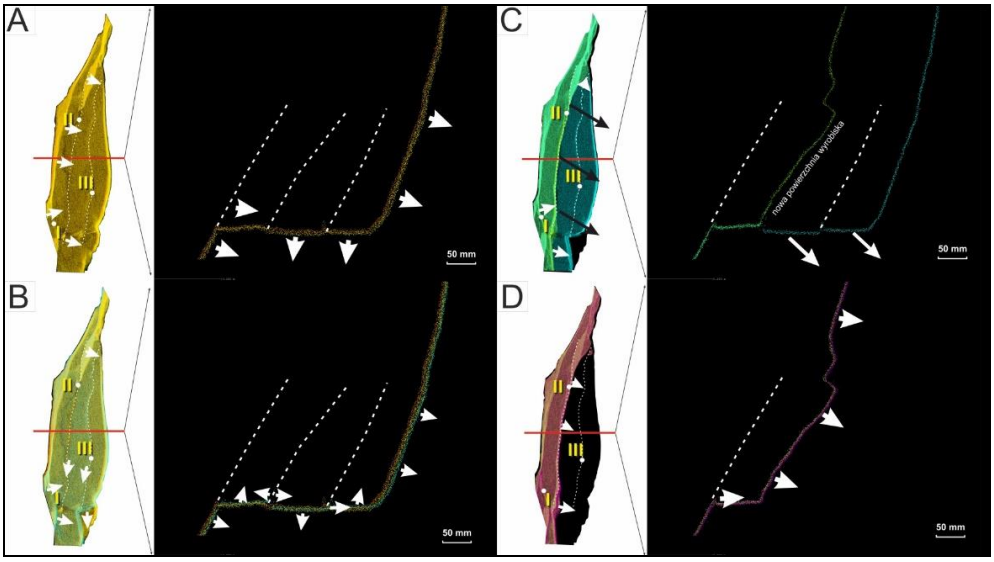

Fig. 4. Cross-sections through the zone of induced fractures made on the basis of differential images from scanning indicating the kinematics of displacements (see explanation in the subsection *Measurements and results – induced fractures*)

5.2. TECTONIC ELONGATED-HELICOIDAL ASYMMETRIC GOUGE (TEHAG)

In the second site (Fig. 5), due to scanning, a "channel shape" tectonic structure within banded dolomite was identified and documented. Analysis of the point cloud made possible to determined and trace its course on the adjacent sidewalls, as well as to approximate orientation of its axis and edges, and measure its width. The measurements of the fracture surfaces within the gouge and its vicinity were made with geological compass first. Scanning was carried out in two measurement series with time frame of two months apart.

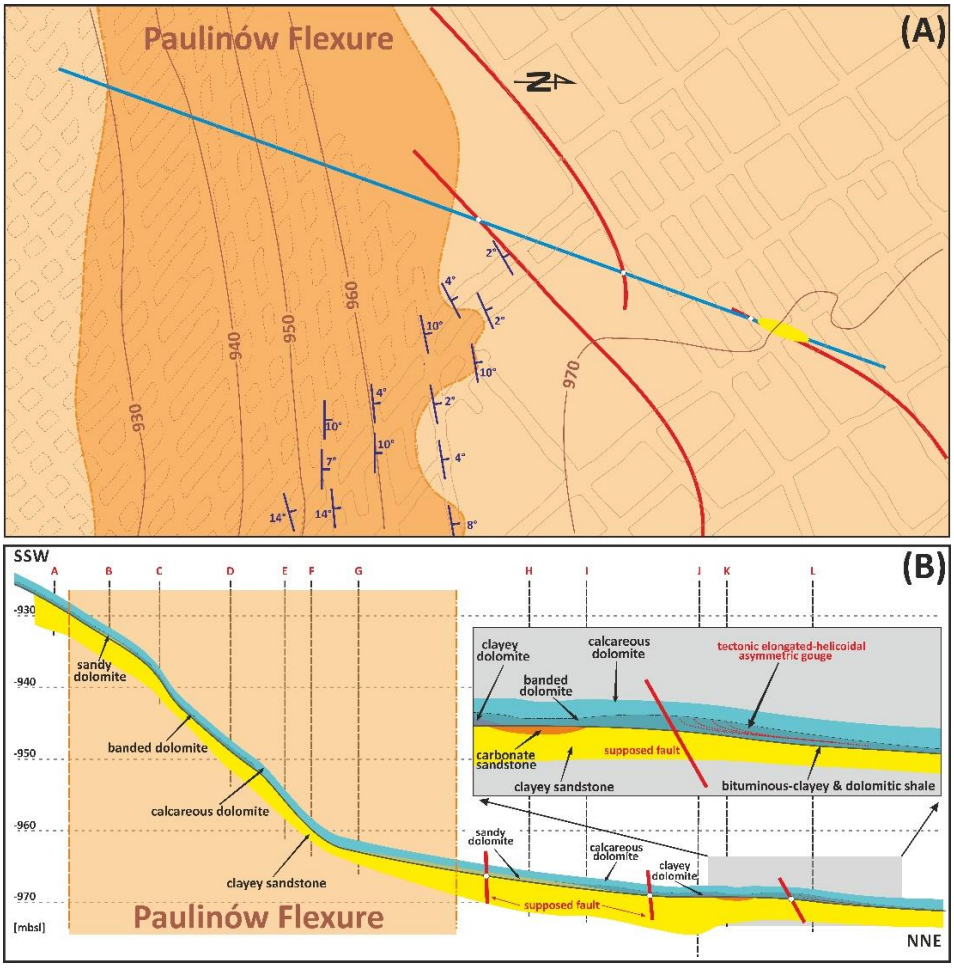

Fig. 5. Location of here described tectonic elongated-helicoidal asymmetric gogue (TEHAG) within the banded dolomites. Inclination of the top surface of the Weissliegend against the background of mine workings and the location of documented and presumed faults (A); geological cross-section of the exploitation level with marked lithology and location of TEHAG (B)

No significant differences between the measurements were observed within the analyzed surfaces produced from the point clouds. The name tectonic elongated-helicoidal asymmetric gouge (TEHAG) used here is a working name (for extensive discussion see Doblas et al. 1997; Doblas 1998; Dżułyński and Kotlarczyk 1965; Tjia 1964; 2014).

The structure occurs in the lower part of the banded dolomite, but the deformation phenomenon also includes the adjacent rocks. Its size is determined by greatest thickness in the axial section H = 69 cm, the greatest width perpendicularly to the axis – W = 465 cm. The structure is elongated and follows in NNE–SSW direction. In the first description of the geometry gouge shape seemed to be cylindrical, however, a detailed assessment of its extent and measurement of this structure with a laser scanner allows it to be distinguished as a surface composed of two, almost symmetrical segments of a helicoid (Fig. 6).

The internal infill of the TEHAG is complex and consists of smaller units – rock fragments with a shape similar to the shape of whole gouge itself, but much smaller in size (H = 5–12 cm, W = 16–41 cm, respectively) and their axes are parallel to the axis of the entire structure. Locally parallel tectonic striation occurs both on the gouge walls and on the walls of the minor internal blocks. In the close vicinity of the gouge, there are low-angle Riedel cracks, suggesting the relative direction of sinistral move on the north-western wall and, on the contrary, dextral ones on the south-eastern wall of the gouge. Oriented thin sections were made in perpendicular cut to the axis of the gouge structure. Unfortunately, the microscopic image turned out to be unreadable in reference to its use to estimate the direction of rock displacement.

6. DISCUSSION

6.1. INDUCED FRACTURES

The stages of the development of induced fractures damaging the corner of the pillar, presented in successive measurement series, allowed observation of the failure process. The authors' observations clearly indicate that in the KGHM mines this process is dependent on the lithology. For mine workings built of homogeneous lithological sections, as is the case of the analyzed site (Site 1), built predominantly of anhydrite sandstone, which is a hard, firm and consolidated rock, the failure caused by the development of induced fractures is of a slightly different nature (e.g. than in rocks with argillaceous cement). The fracture surface between Blocks I and II as well as II and III is characteristically concave in the upper part. This corresponds to the geometry of the fracture surfaces observed within the anhydrite sandstone at this site. The destruction probably occurs as a result of rockfall, sometimes induced by natural or artificial seismic events. Ollier (1978) was first, who described this type of fracture in granitic rocks found in South Australia, in which a much wider, upper part of the object is

pressed against the base of the rock formations. At the base, there is a break-off of the rock fragment along the concave surface of the fracture. The rounded shape of this surface is a result of the spherical form that the object rock had. In the case of the analyzed site, the shape of the surface of the fractures also results from the form in which they occur – they follow the shape of the mine workings' wall.

On the other hand, the geometry and density of the fracture surfaces varies depending on which profile of the ore zone they occur in. Moreover, within a single profile, these features are mostly variable, especially if a thick shale layer (characterized by additional internal anisotropy) is present in the profile between the dolomite and sandstone. Due to its relatively small thickness and clear distinctiveness from higher and lower lithological horizons, fractures do not continue from the sandstone through the shale into the dolomite. While in the case of a pillar corner at the analyzed site the fracture surfaces develop along one of the walls of the corner, for workings with a typical profile of the ore zone the fracture surfaces often cut the pillar corners obliquely.

Sedimentological determinants affecting the development of induced fractures and the damage to pillars are further effected by mining conditions. The rate of development of induced fractures is definitely different within mining fields, where pillars are cut to small dimensions and the convergence of workings is very high (even up to 0.5 m per week). These workings, however, are relatively quickly liquidated and closed off from use, i.e., the presence of people and mining equipment within them. However, there are many other types of mine workings, e.g., transport, haulage, ventilation, or providing access to new areas of the deposit, which must be maintained over a long, often multi-year time frame. Different rates of development of induced fractures should be expected in pillars located within the excavations running along goafs (mined out and liquidated fields) and different in mine openings, which run far into the rock mass and are not yet adjacent to the mining fields. The authors collected data from sites located in several different geologic-mining situations, which require further works of analysis and interpretation.

The collection of such a large amount of diverse data would not have been possible without the use of terrestrial laser scanning, which has proven to be a very effective tool for acquiring high-quality, extremely precise spatial data. The advantages of these devices are appreciated and used in many fields, including mining, as they allow not only precise measurements of objects and structures, but also to mapping and visualization of these structures in three-dimensional space. Also in geological applications, laser scanning has played an important role for many years (e.g., Buckley et al. 2008). It is impossible to imagine modern geologic mapping without lidar images (e.g., Jagodnik et al. 2020; Kowalski and Wojewoda 2016; Lo et al. 2021), nor is monitoring of areas most threatened of landslides (e.g., Jaboyedoff et al. 2012, Sikora and Wojciechowski 2019; Waga and Fajer 2021). However, the use of laser scanners for geological documentation in underground mines offers new possibilities for data analysis and visualisation. In many districts of the Rudna mine, underground workings have difficult working conditions.

Laser scanning makes it possible, first of all, to quickly and efficiently record entire lines of mine workings, and then analyze the acquired material in safe office conditions. The tests carried out in the second site indicate that properly prepared data allows documentation of structural phenomena, especially in hard-to-reach parts of the workings. This is supported by the authors' observations based on the analysis of scanning data from other sites in the Rudna mine (Sokalski et al. 2019; 2020). With appropriate filtering and visualization of the data, it is also possible to distinguish some lithological sections. In addition, the sites can be conveniently viewed in full three-dimensional space from different perspectives and in a wide spectrum of colors, which makes it possible to discover details that would be very difficult to see when documenting the sites in the conventional way. The analysis of differential images (scans) used by the authors to observe the development of induced fractures further supports the interpretation of phenomena developing over time. It should be noted that aligning scans from substations is subject to error, which is about 2–3 mm in both sites. In addition, aligning scans from individual measurement series into a differential scan also has a registration error. For the second site, the registration error (expressed as standard deviation) is 4 mm. Some measured displacement values (Fig. 4) are more than 10 mm (even up to 15 mm). Thus, it can be assumed that the recorded displacements exceed the calculated error, but indicating unambiguous values requires analysis of more data.

Before conducting measurements, the authors performed tests to select the optimal scanning parameters for structural analysis. The goal was to achieve the highest possible measurement accuracy for which the scanning time of one several-meter-long section of mine working took an average of about 45 minutes (with moving and setting up the equipment between sub-stations). Depending on the needs of the surveyor, this time could be reduced at the expense of data quality (density). The authors' experience shows that for the purpose of preliminary documentation of the state of the mine workings for subsequent geological analysis (not involving analysis of sub-millimeter displacements), the measurement time can be reduced by up to three times, allowing a significant improvement in work efficiency. Such an approach was applied to site no. 2 by reducing the frequency of the laser beam from 1200 kHz to 600 kHz, and the results were sufficient to obtain high enough quality documentation of the site.

The amount of data collected by the authors is a result of the goal of the measurements, which was to record changes occurring on a sub-millimeter scale. The authors made a compromise on the measurement time, which directly reflects on the resolution of the scans, in order to record the destruction process caused by the development of non-tectonic induced fractures as accurately as possible. The authors agree that an experienced geologist is necessary to analyze such specific structural features and their geokinematics. However, they see the possibility of simplifying the measurement and analytical-interpretation process for more general characterization of mine workings deformation on a more regional scale, where high precision/resolution is not crucial to indicate trends.

Interpretation of structural features of the rock mass can also be developed from the point cloud in a more automated manner. Algorithms for automatic and semi-automatic detection of discontinuity surfaces have been successfully used for several years now for large outcrops that are difficult to access or pose a danger to the person taking the measurements. This type of automation is increasingly being conducted in geotechnical documentation, e.g., for structures or infrastructure objects prone to geo-hazards (e.g., Sturzenegger and Stead 2009; Lato et al. 2009; Vöge et al. 2013; Chen et al. 2018; Riquelme et al. 2019; Pan et al. 2019; Kumar Singh et al. 2023). Due to the different purpose of the authors' research, the tools enabling automation of interpretation procedures were not used in this paper.

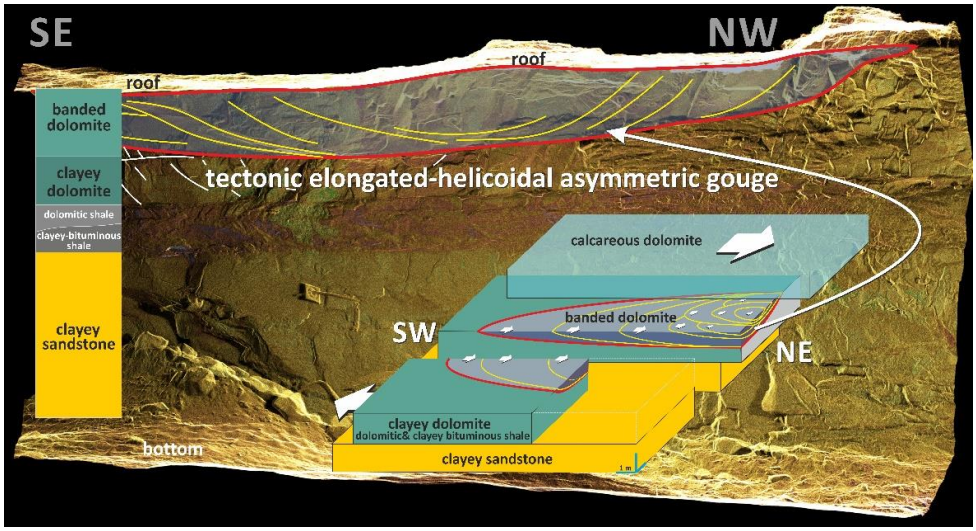

Fig. 6. Tectonic Elongated-Helicoid Asymmetric Gouge (TEHAG) within banded dolomites. Laser scan image (background), lithological profile (left) and spatially oriented model of formation of the TEHAG

6.2. TECTONIC ELONGATED-HELICOIDAL ASYMMETRIC GOUGE (TEHAG)

Laser scanning also reveals its usefulness in documenting structures formed long before the rock mass was cut by excavations and mining operations. The gouge structure was identified in the three-dimensional image created from the point cloud by applying the effect of point transparency and using an appropriate color gradient to color the point cloud according to reflectance value. In this particular case, the experience of the geologist analyzing the cloud image was equally important to correctly identify the boundaries of the structure and the shape of the fracture planes within it. This may be an important premise for further paleotectonic considerations. No displacements were recorded in the differential image. This corresponds to authors' observations, which

indicate that the analyzed structure is old and reactivated in the sidewall as a result of the exploitation process. The authors find it unlikely that recent geodynamic phenomena are associated with this structure. In order to confirm these observations, however, several additional measurement series should be made over longer time interval. The gouge structure most probably documents a mechanism of "chipping off" and rebuilding a fragment of the subsoil during horizontal overthrusts in the rock mass. Considering its position in relation to other elements of local and supra-local tectonics (cf. Fig. 5), a working thesis can be put forward that it is part of the fractal nature of many structural phenomena. Further microstructural studies are required, because those carried out by the authors have been limited to only few oriented microscopic preparations, unfortunately without success.

The EHAG structure in its present orientation does not directly refer to the Middle Odra Fault Zone. The scanning results show that it is a dead (frozen?) structure, which was formed much earlier than the recent and contemporary geokinematic activity of this area. This may indicate, for example, a significant structural reconstruction of this part of the Fore-Sudetic Homocline. It can be postulated that the present orientation and spatial position of the currently observed tectonic phenomena should be corrected backwards, and interpreted in a paleogeographic context rather than in a present day rock architecture.

7. FINAL REMARKS AND CONCLUSIONS

Recognizing structural phenomena observed in mine workings is among the tasks carried out by mine geologists. Not only data on the structure of the rock mass, but most of the information and data provided by geologists often constitutes the basis for other mine services. The results obtained by the authors prove that the data acquisition process can be assisted using modern methods as terrestrial laser scanning. Especially since the laser scanner acquires data that can be independently used in many other fields, by geologists, mining engineers and mine surveyors. The development of a suitable methodology for data acquisition can significantly facilitate and improve the work of various mine services.

The authors present analysis of the development of induced fractures and unique tectonic phenomena within the mine workings, which is a preliminary step to the construction of a model that allows the prediction of geodynamic behavior of the rock mass. The ongoing progress of laser scanning technology already makes it possible to state that presented methods for structural documentation can be further improved and take a step further – towards consistent and full-scale monitoring of mine geohazards.

Mine trucks are covering tens of kilometers every day through hundreds of kilometers of workings located in the Rudna mine. Combined with mobile scanning technology, it is possible to scan entire lines of crucial mine workings. Developing an appropri-

ate monitoring methodology, especially in terms of optimal management of the huge amount of data obtained from scanning (order of terabytes), can improve the safety of mining, not only in terms of geohazards, but also allows to record phenomena "invisible" to classical field methods of documentation of the mine workings.

However, even despite the use, or adapting, of new technologies to assist in the mining process, the conceptual work of geologists is essential to solve today's encountered risks. Geodynamic, gas, or hydrogeological hazards will appear and intensify as the mining front progresses. Recognizing the structure of the rock mass and providing correct description of the phenomena are essential for recognizing the processes driving them and possibly counteracting the harmful effects. Particularly important for safety and correct decisions on planning the progress of mining work is the recognition of the structure of the rock mass made just after it has been preliminarily explored and opened for exploitation. Currently, the preliminary reconnaissance, so typical in the first years of opening the deposit, "weakened" after the mining front passed through the mining fields located within and adjacent to the main tectonic structures. As mining work progresses, new mining fields are being accessed, currently in the central and northern parts of the mining area, where the nature of previously identified structures is changing or new, previously unknown structures are being revealed, such as the TEHAG structure described in this paper. Over the past several years, many new concepts of geologic space and surfaces have emerged that can change the understanding of structural phenomena. The use of laser scanning offers new quality and possibilities in documenting geological sites, but also makes it possible to view geologic space in three dimensions, enabling perception that the planes of fractures or faults are 3D structures.

ACKNOWLEDGEMENTS

The authors would like to thank Dr. Weronika Gorczyk for her technical and substantive comments on the paper, to Dr. Damian Kasza and Dr. Jarek Wajs, and to Jacek Krawiec and Klaudia Gergont of Laser-3D for their invaluable help in taking measurements.

REFERENCES

BUCKLEY S.J., HOWELL J.A., ENGE H.D., KURZ T.H., 2008, *Terrestrial laser scanning in geology: data acquisition, processing and accuracy considerations*, Journal of the Geological Society, 165 (3), 625–638.

CHEN S., WALSKE M.L., DAVIES I.J., 2018, *Rapid mapping and analysing rock mass discontinuities with 3D terrestrial laser scanning in the underground excavation*, International Journal of Rock Mechanics and Mining Sciences, 110, 28–35.

DRONSZCZYK P., STRACH M., 2016, *Zastosowanie technologii skaningu laserowego i termowizji do inwentaryzacji tunelu i znajdujących się w nim urządzeń przeciwpożarowych*, Bezpieczeństwo i Technika Pożarnicza, 43 (3), 199–214.

DUMICZ M., DON J., 1977, *Analiza strukturalna monokliny przedsudeckiej w regionie Polkowic*, Acta Univ. Wratisl., 378, Pr. Geol.-Min., 6, 279–302.

DUSZA-PILARZ K., KIREJ M., 2019, *Wykorzystywanie skaningu laserowego oraz oprogramowania 3D w projektowaniu górniczym*, KGHM Polska Miedź SA O/ZG Rudna. Materiały konferencyjne XXVIII Szkoły Eksploatacji Podziemnej w Krakowie, 25–27.02.2019 r.

DOBLAS M., MAHECHA V., HOYOS M., and LOPEZ-RUIZ J., 1997, *Slickenside and fault surface kinematic indicators on active normal faults of the Alpine Betic Cordilleras, Grenada, southern Spain*, Journal of Structural Geology, 19, 159–170.

DOBLAS M., 1998, *Slickenside kinematic indicators*, Tectonophysics, 295, 187–197.

DŻUŁYŃSKI S. and KOTLARCZYK J., 1965, *Tectoglyphs on slickensided surfaces*, Bulletin de l'Academie Polonaises des Sciences, Serie Geologie et Geographie, 17, 149–154.

JABOYEDOFF M., OPPIKOFER T., ABELLÁN A., DERRON M.-H., LOYE A., METZGER R., PEDRAZZINI A., 2012, *Use of LIDAR in landslide investigations: a review*, Nat. Hazards, 61, 5–28.

JAGODNIK P., GAZIBARA S.B., ARBANAS Ž., MIHALIĆ ARBANAS S., 2020, *Engineering geological mapping using airborne LiDAR datasets – an example from the Vinodol Valley, Croatia*, Journal of Maps, 16 (2), 855–866.

KACZMAREK W., 2006, *Zróżnicowanie mineralizacji miedziowej a wykształcenie litologiczne białego spągowca w kopalniach LGOM*, Rozprawa doktorska, Arch. Inst. Nauk Geol. Uniw. Wroc.

KACZMAREK W., TWARDOWSKI M., WASILEWSKA-BŁASZCZYK M., 2017, *Praktyczne aspekty modelowania litologicznych typów rud w złożach Cu-Ag LGOM (Legnicko-Głogowskiego Okręgu Miedziowego)*, Biuletyn PIG, (468), 209–226.

KARNKOWSKI P.H., 2007, *Permian Basin as a main exploration target in Poland*, Przegląd Geologiczny, 55 (12/1), 1003–1015.

KIERSNOWSKI H., 1995, *Geneza i rozwój późnopaleozoicznego wschodniego basenu przedsudeckiego*, [w:] S. Cwojdziński i in. (red.), *Geologia i Ochrona Środowiska Bloku Przedsudeckiego*. Materiały Sesji LXVI Zjazdu PTG, Ann. Soc. Geol. Polon., wydanie specjalne, 19–35.

KIERSNOWSKI H., PERYT T.M., BUNIAK A., MIKOŁAJEWSKI Z., 2010, *From the intra-desert ridges to the marine carbonate island chain: middle to late Permian (Upper Rotliegend – Lower Zechstein) of the Wolsztyn–Pogorzela high, west Poland*, Geological Journal, Vol. 45, 319–335.

KŁAPCIŃSKI J., KONSTANTYNOWICZ E., SALSKI W., KIENIG E., PREIDL M., DUBIŃSKI K., DROZDOWSKI S., 1984, *Atlas obszaru miedzionośnego (monoklina przedsudecka)*, Wyd. „Śląsk", Katowice.

KONSTANTYNOWICZ E. (red.), 1971, *Monografia przemysłu miedziowego w Polsce*, Wydawnictwa Geologiczne, Warszawa, 1–432.

KOWALSKI A., WOJEWODA J., 2016, *Obrazy lidarowe – przetwarzanie i zastosowanie w geologii*, [in:] D. Olszewska-Nejbert, A. Filipek, M. Bąbel, A. Wysocka (red.), VI Polska Konferencja Sedymentologiczna POKOS 6. Chapter: *Materiały do warsztatów*, Instytut Geologii Podstawowej Wydziału Geologii Uniwersytetu Warszawskiego.

KUMAR SINGH S., PRATAP BANERJEE B., RAVAL S., 2023, *A review of laser scanning for geological and geotechnical applications in underground mining*, International Journal of Mining Science and Technology, 33 (2), 133–154.

KUMOSIŃSKI W., PATYKOWSKI G., 2020, *Doświadczenia ze skanowania i modelowania 3D wyrobisk górniczych KGHM Polska Miedź SA, O/ZG „Lubin"*. KGHM Polska Miedź SA, O/ZG „Lubin". Materiały konferencyjne z XXIX Szkoły Eksploatacji Podziemnej w Krakowie, 24–26.02.2020 r.

LATO M., DIEDERICHS M.S., HUTCHINSON D.J., HARRAP R., 2009, *Optimization of LiDAR scanning and processing for automated structural evaluation of discontinuities in rockmasses*, International Journal of Rock Mechanics and Mining Sciences, 46 (1), 194–199.

LO P.-C., LO W., WANG T.-T., HSIEH Y.-C., 2021, *Application of Geological Mapping Using Airborne-Based LiDAR DEM to Tunnel Engineering: Example of Dongao Tunnel in Northeastern Taiwan*, Applied Sciences, 11 (10), 4404, 19 pp.

MARKIEWICZ A., ALEKSANDROWSKI P., CZARNECKA K., DOKTÓR S., GRANICZNY M., 1995, *Tektonika a rozkład naprężeń pierwotnych i wtórnych w obszarze „ZG Rudna”*, Arch. CBPM Cuprum, Wrocław.

MARZEC M., PATYKOWSKI G., KUMOSIŃSKI W., 2016, *Monitoring deformacji podziemnych wyrobisk górniczych KGHM PM S.A. O/ZG „Lubin” z wykorzystaniem technologii skaningu laserowego*, KGHM Polska Miedź S.A. Materiały konferencyjne z XXV Szkoły Eksploatacji Podziemnej w Krakowie, 22–26.02.2016 r.

NEUENDORF K.K.E., MEHL J.P., Jr., and JACKSON J.A. (eds.), 2011, *Glossary of Geology*, Alexandria, Virginia, American Geological Institute, 799 p.

NEMEC W., PORĘBSKI S., 1977, *Weissliegendes sandstones: a transition from fluvial-aeolian to shallow-marine sedimentation (Permian of Fore-Sudetic Monocline)*. 2. *A study in significance of rock colouration*, Rocznik PTG, 47, 513–544.

OBERC J., 1967, *Budowa tektoniczna terenów XL Zjazdu PTG w Zgorzelcu*, Przegl. Geol., 15 (6), 253–262.

OBERC J., 1972, *Budowa geologiczna Polski*, t. IV. *Sudety i obszary przyległe*, Wyd. Geol., Warszawa, 1–307.

OLLIER C., 1978, *Induced fractures and granite landforms*, Zeitschrift für Geomorphologie, 22 (3), pp. 249–257.

OSZCZEPALSKI S., 1999, *Origin of the Kupferschiefer polymetallic mineralization in Poland*, Miner. Depos., 34 (5–6), 599–613.

OSZCZEPALSKI S., 2007, *Paleogeografia obszaru złożowego monokliny przedsudeckiej*, [w:] A. Piestrzyński (red.), *Monografia KGHM Polska Miedź S.A.*, Lubin, 104–107.

PAN D., LI S., XU Z., ZHANG Y., LIN P., LI H., 2019, *A deterministic-stochastic identification and modelling method of discrete fracture networks using laser scanning: Development and case study*, Engineering Geology, 262, 105310.

PAPIERNIK B., GÓRECKI W., PASTERNACKI A., 2010, *Wstępne wyniki modelowań przestrzennych (3D) parametrów petrofizycznych skał podczas poszukiwań stref występowania gazu zamkniętego w polskim basenie czerwonego spągowca*, Przegląd Geologiczny, 58 (4), 352–364.

PATYKOWSKI G., KUMOSIŃSKI W., 2014, *Skanowanie wyrobisk górniczych w warunkach KGHM Polska Miedź S.A. Oddział Zakłady Górnicze „Lubin”* (*Scanning of tunnels in KGHM Polska Miedź S.A. Oddział Zakłady Górnicze „Lubin”*), KGHM Polska Miedź S.A. Materiały konferencyjne z XXIII Szkoły Eksploatacji Podziemnej w Krakowie, 24–28.02.2014 r.

PATYKOWSKI G., MARKIEWICZ Ł., MŁYNARCZYK J., OLSZEWSKI S., 2013, *Wykorzystanie technologii TLS do budowy trójwymiarowego modelu wyrobisk górniczych KGHM PM S.A*, KGHM POLSKA MIEDŹ S.A. Materiały konferencyjne z XXII Szkoły Eksploatacji Podziemnej w Krakowie, 18–22.02.2013 r.

PERYT T.M., 1978, *Wykształcenie mikrofacjalne dolomitu głównego w północnej części monokliny przedsudeckiej*, Przegl. Geol., 26 (3), 163–168.

PIESTRZYŃSKI A. (red.), 1996, Monografia KGHM Polska Miedź S.A., Lubin, 1220 pp.

PIESTRZYŃSKI A. (red.), 2007, Monografia KGHM Polska Miedź S.A., Lubin, 1080 pp.

PIESTRZYŃSKI A., WODZICKI A., 2000, *Origin of the gold deposit in the Polkowice-West mine, Lubin-Sieroszowice Mining District, Poland*, Miner. Deposita, 35, 37–47.

RIQUELME A., TOMÁS R., CANO M., PASTOR J.L., ABELLÁN A., 2018, *Automatic Mapping of Discontinuity Persistence on Rock Masses Using 3D Point Clouds*, Rock Mech. Rock Eng., 51, 3005–3028.

SALSKI W., 1975, *Tektonika okolic Lubina*, Biul. Inst. Geol., 287, 61–178.

SELEROWICZ, 2011, *Synklina Paulinowa na terenie ZG „Rudna”*, Praca magisterska, Wydział Nauk o Ziemi i Kształtowania Środowiska, Uniwersytet Wrocławski.

SIKORA R., WOJCIECHOWSKI T., 2019, *Osuwiska w Sudetach*, Przegląd Geologiczny, 67 (5), 360–368.

SLAKER B.A., 2015, *Monitoring Underground Mine Displacement Using Photogrammetry and Laser Scanning*, PhD Dissertation, Virginia Polytechnic Institute and State University.

SOKALSKI D., 2022, *Development of Mining Induced Fractures Documented with Terrestrial Laser Scanner – an Example from Rudna Copper Mine, Poland*. Book of abstracts XXII Conference of PhD Students and Young Scientists, June 29–July 1, 2021.

SOKALSKI D., WOJEWODA J., KASZA D., WAJS J., 2019, *Tectonic Structures Related to Paulinów Syncline in Rudna Copper Mine, Poland Documented with Terrestrial Laser Scanner*. Book of Abstracts 20th Czech-Polish Workshop on Recent Geodynamics of Central Europe, 24–26 of October 2019, Szklarska Poręba.

SOKALSKI D., WOJEWODA J., KOWALSKI A., 2020, *Epigenetic and Induced Fractures from the Radków Bluff (Stołowe Mountains) Documented with Terrestrial Laser Scanner – Structural Implications*. Book of abstracts XX Conference of PhD Students and Young Scientists, October 14–16, 2020.

STURZENEGGER M., STEAD D., 2009, *Close-range terrestrial digital photogrammetry and terrestrial laser scanning for discontinuity characterization on rock cuts*, Engineering Geology, 106 (3–4), 163–182.

ŚLIWIŃSKI W., 2000, *Rozwój mineralizacji miedziowej w utworach permu monokliny przedsudeckiej – uwarunkowania sedymentacyjno-diagenetyczne*, Acta Univ. Wratisl., 2197, Pr. Geol. Miner., 68, 7–36.

TJIA H.D., 1964, *Slickensides and fault movements*, Bulletin Geological Society of America, 75, 683–686.

TIJA H.D., 2014, *Fault-Plane Markings as Displacement Sense Indicators*, Indonesian Journal on Geoscience, 1, 151–163.

TWARDOWSKI M., 2023, *Geostatystyczne modele zmienności parametrów złoża rud miedzi monokliny przedsudeckiej w kluczowych domenach geologicznych*, Rozprawa doktorska, Akademia Górniczo-Hutnicza im. Stanisława Staszica w Krakowie.

VAN WEES J.-D., STEPHENSON R.A., ZIEGLER P.A., BAYER U., MCCANN T., DADLEZ R., GAUPP R., NARKIEWICZ M., BITZER F., SCHECK M., 2000, *On the origin of the Southern Permian Basin, Central Europe*, Marine and Petroleum Geology, Vol. 17, Iss. 1, January, 43–59.

VAUGHAN D. J., SWEENEY M., FRIEDRICH G., DIEDEL R., HARAŃCZYK C., 1989, *The Kupferschiefer: An Overview with an Appraisal of the Different Types of Mineralization*, Econ. Geol., 84 (5), 1003–1027.

VÖGE M., LATO M., DIEDERICHS M.S., 2013, *Automated rockmass discontinuity mapping from 3-dimensional surface data*, Engineering Geology, 164, 155–162.

WAGA J.M., FAJER M., 2020, *Formy osuwiskowe w południowo-zachodniej części Kotliny Oświęcimskiej – rozmieszczenie i uwarunkowania rozwoju*, Unpublished, Arch. UŚ.

WOJEWODA J., OLLIER C., 2012, *Origin of selected fractures within Cretaceous sandstones in the Table Mountains*, Posiedzenia Naukowe PTG, Wrocław, 29.11.

ŻELAŹNIEWICZ A., ALEKSANDROWSKI P., BUŁA Z., KARNKOWSKI P.H., KONON A., OSZCZYPKO N., ŚLĄCZKA A., ŻABA J., ŻYTKO K., 2011, *Regionalizacja tektoniczna Polski*, Kom. Nauk Geol. PAN, Wrocław, 60 pp.